IEEE Access
Multidisciplinary : Rapid Review : Open Access Journal

Received September 8, 2018, accepted September 27, 2018, date of publication October 15, 2018,
date of current version November 14, 2018.

Digital Object Identifier 10.1109/ACCESS.2018.2875972

Multi-Objective Optimization of VSC Stations in Multi-Terminal VSC-HVdc Grids, Based on PSO

ALI RAZA[1], ZAIN YOUSAF[1], MOHSIN JAMIL[1,2], SYED OMER GILANI[1], GHULAM ABBAS[3], MUHAMMAD UZAIR[2], SAIMA SHAHEEN[4], ABDELDJABAR BENRABAH[5], AND FAJUN LI[6]

[1]Department of Robotic and AI, National University of Sciences and Technology, Islamabad 44000, Pakistan
[2]Department of Electrical Engineering, Islamic University of Madinah, Madinah 41411, Saudi Arabia
[3]Department of Electrical Engineering, The University of Lahore, Lahore 54000, Pakistan
[4]Department of Electrical Engineering, University of Management and Technology, Lahore 54000, Pakistan
[5]Department of Electrical Engineering, Ecole Militaire Polytechnique, Algiers 16000, Algeria
[6]Department of Electronic Science and Technology, Harbin Institute of Technology, Harbin 150001, China

Corresponding author: Ali Raza (i.will.rize@gmail.com)

ABSTRACT The objective of this paper is to enhance the control performance of voltage source converter (VSC) stations within multi-terminal high voltage direct current (M-HVdc) grids under dynamic conditions. This paper presents the application of particle swarm optimization (PSO) to tune the control parameters of VSC stations. VSCs are non-linear components of the M-HVdc grids. Conventional techniques use approximated linear models to tune the control parameters which do not produce optimal results. Thus, PSO is employed to optimally tune the control parameters of VSC stations. The algorithm of the proposed objective function applies simultaneous optimization of inner and outer control layers. Dynamic simulations of a four-terminal HVdc system are developed in PSCAD/EMTDC to extol the merits of the presented optimization technique. Results show the steady state and dynamic control performances, both for classically and PSO-based tuned parameters, during load demand change from ac grids, wind power change, and eventual permanent VSC disconnection.

INDEX TERMS Multi-terminal VSC-HVdc grid, multi-objective optimization, offshore wind farms, particle swarm optimization (PSO), voltage source converters, proportional integral (PI).

I. INTRODUCTION

Recent research shows that to meet the future network requirements, multi-terminal high voltage direct current (M-HVdc) has emerged as the promising solution. Multi-terminal dc grids not only have significant advantages but have emerged with some favorable applications [1], [2]. These include the integration of offshore wind farms into mainland ac grids [3], thus the proposed European super grid [4], and the encouraging possibility of the interconnection of North Sea wind farms with Scandinavian hydropower and Mediterranean solar plants [2]. The multi-terminal high voltage dc system avoids capacitance currents, compared with those with long cable ac transmission.

In the near future M-HVdc grids will provide robust and flexible controlled infra-structures [5]. This will compel the power system and power electronics companies to develop such control strategies to increase system reliability, security, and efficiency [6].

With the latest developments in the voltage source converter (VSC)-HVdc technology, research show that the feasibility of connecting the high voltage dc power system, using multiple power converter stations, is possible with appropriate control [7]. VSC-HVdc appears a suitable tool for M-HVdc grid construction, with manufactured M-HVdc grids based on VSC reported in [8] and [9].

VSC-HVdc station control is based on the flux-oriented vector current control (VCC) technique. It has two control layers: an inner current control (ICC) layer and outer control layer (OCL) [10]. The outer layer achieves its goal by guiding the active power, reactive power, dc voltage or ac voltage control to VSCs, based on the requirements of the connected ac grid. Whereas, inner current control loop regulates the d-axis and q-axis current variables by using a decoupling control strategy. Both of these loops have an important element in common: a proportional and integral (PI) controller. Voltage droop control is frequently adopted to regulate the dc-link voltages in a precise range and power sharing within the grid, applied in the outer layer [3], [6]. After investigating the interconnecting control layers of the M-HVdc grid, the VSC-station is a complex multi input and multi output control system [7], [11]. This complex structure has numerous variables, which needs strong yet simple control; using

PI controllers [3], [12]. Thus, the corresponding PI parameters should be optimally tuned and adjusted, which improves both steady state and transient performance. However, it is challenging to properly tune the gains of PI controllers for nonlinear systems (for example, a voltage source converter) [13], [14]. Classically proposed tuning methods face difficulties in determining the near optimal or optimized PI parameters [15]. Conventional techniques use approximate linear models to tune the PI control parameters, but VSCs are non-linear in nature which does not produce optimal results [16]. Different computerized mathematical models have been implemented to deal with the nonlinearities of the dc grids. However, performance based on such models results in mis-convergence during dynamic behavior [17].

Genetic algorithm (GA), computational intelligence approach, discussed in [18] and [19] to improve the system performance by tuning the controller's parameter. Thus the heuristic techniques are good candidate to deal with systems having nonlinearities. However, performance of GA is limited because it exhibits slow convergence towards the solution as GA has to perform three operations namely; selection, crossover and mutation in each iteration [17]. Thus optimized tuning of PI control parameters is a challenge and a meta-heuristic technique based on particle swarm optimization (PSO) is proposed to deal with the mentioned shortcomings [20].

VSC stations need a precise and efficient output during any disturbance, but achieving this task is time consuming and lengthy process. Particle swarm optimization (PSO) application assists solving the problem. Kennedy and Eberhart [20] proposed PSO in 1995; robustness in dealing with non-linear problems efficiently. Thus a PSO algorithm based PI controller becomes effective and show better results in a shorter time. Evidence shows that the PSO technique has solved various powers system problems efficiently [21], [22].

In this research, an optimized control structure using the multi-objective PSO algorithm is proposed and investigated. To the best of author's knowledge, multi-objective PSO has not been employed to improve VSC response within an M-HVdc grid. Dynamic simulations for a four-terminal VSC-HVdc transmission system are developed in PSCAD/EMTDC to validate the merits of the presented optimization technique.

Two parallel sets of PI controllers operating in the inner and outer loops simultaneously are optimized using multi-objective PSO to achieve an optimized control structure. Simulations developed both for C-PI and PSO-PI are assessed for steady state and dynamic control performance during (i) load demand change from ac grids, (ii) wind power change, and (iii) eventual permanent VSC disconnection.

II. PROPOSED M-HVdc TEST SYSTEM AND CONTROL LAYOUT

A single line diagram of modular multi-level converter (MMC) based four terminal test system is shown in Fig. 1.

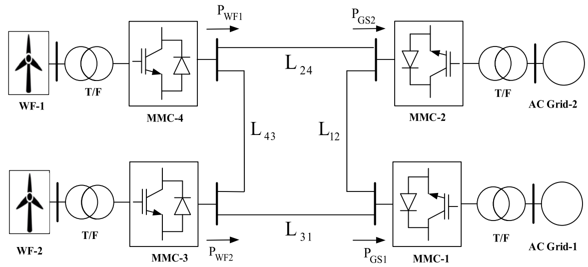

FIGURE 1. Single line diagram of four terminal MMC-HVdc transmission system composed of two wind farms and two onshore ac networks.

Bi-polar transmission cables are connected via negative and positive dc voltages. DC inductors (100mH) are included in each line to mimic a practical dc system. However, these inductors do not come with protection against dc grid faults. Length of each line is 100km and ratings of the dc test system are given in Table 1.

TABLE 1. Four terminal MMC-HVdc test gird parameters.

	Nominal voltage	Impedance	Specifications
Wind farms	33kV	0.002 + j0.01p.u.	1000MW
ac- networks	230kV	0.001 + j0.015p.u.	1000MW
dc capacitor	400kV	Two 1400µF capacitors in series	-
dc-link	400kV	R= 0.10 x 10^{-3} Ω/km L= 0.50 x 10^{-3} H/km C= 2.31 x 10^{-7} F/km	100km between all VSC stations

The M-HVdc control, with the dc voltage control at VSCs, active and reactive power control with ac voltage regulation at the point of common coupling (PCC). For this purpose, vector current control is used to regulate the VSC-HVdc stations [23]. In this methodology, the ac currents and voltages of the converter are changed into the rotating *d-q* reference frame, which is phase-locked loop (PLL) synchronized with the ac grid voltages. This strategy gives decoupled control of the active and reactive power and regulates the ac and dc voltages, respectively. The layout of the VSC control using *d-q* control is shown in Fig. 2. The outer controllers produce reference currents for the inner current controller, which then decides the voltage references for the *d-q* reference frame.

A. INNER CURRENT CONTROL (ICC)

Taking into account the d-q frame, the inner current controller incorporates the PI controllers which are responsible for the reference currents and manage the reference voltages for the VSCs. The relation between the voltages at PCC (e_c) and the VSC side (v_g) is given by:

$$e_c - v_g = R \times i_c + L \times \frac{di_c}{dt} \tag{1}$$

where i_c is the current from the ac framework to the converter while R and L represent resistance and inductance between the PCC and the VSC station. By applying

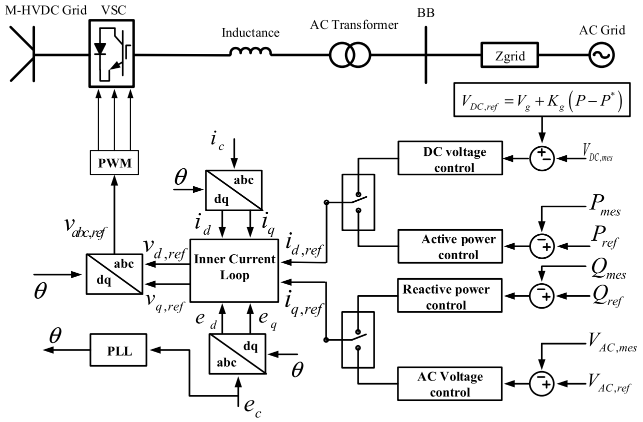

FIGURE 2. The *d-q* control architecture for VSC-HVdc station.

Park transformation:

$$e_d - v_d = Ri_d - \omega L i_q + L \times \frac{did}{dt} \tag{2}$$

$$e_q - v_q = Ri_q + \omega L i_d + L \times \frac{diq}{dt} \tag{3}$$

where ω is the angular frequency at the PCC of the ac system. ICC control layout is shown in Fig. 3 based on (2) and (3). Switching for IGBTs are generated by transforming the reference signals ($v_{d,ref}$ and $v_{q,ref}$) back to the *abc* frame.

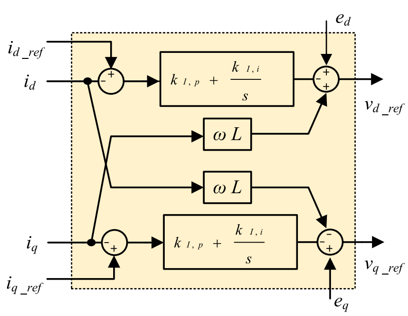

FIGURE 3. Inner current controller structure.

B. OUTER CONTROL LAYER (OCL)

The dc and ac voltage, active and reactive powers at the PCC are controlled by the outer controller. The d-channel controls active power or dc voltage control while the q-channel controls reactive power or ac voltage regulation as shown in the Fig. 2 and mathematically are:

$$P = v_d i_d + v_q i_q \tag{4}$$

$$Q = v_q i_d - v_d i_q \tag{5}$$

The d-axis of the vector control is PLL synchronized with the ac system phasor voltages, thus $v_q = 0$.

$$P = v_d i_d \tag{6}$$

$$Q = -v_d i_q \tag{7}$$

Active and reactive powers are regulated by employing the d-q axis currents as from (6) and (7). The amplitude of the ac voltages at the PCC is controlled via ac voltage controller by injecting the appropriate amount of reactive power into the system such that the PCC ac voltage matches the given reference voltage. Similarly, ac voltage can be regulated by modifying the q-axis current. The dc-link voltage is maintained at its preset reference value via proper real power exchange with ac network. Thus the dc-link voltages can be controlled by modifying the d-axis current.

III. CONTROLLERS OPTIMIZATION BASED ON PARTICAL SAWRM OPTIMIZATION (PSO)

M-HVdc system performance depends on accurate tuning of the PI controllers of the VSC stations. Thus, the optimal tuning of PI parameters is of importance. So, an heuristic algorithm, particle swarm optimization, is employed for control optimization in this paper. As PSO offers advantages like; speedy convergence, simple implementation, and low vulnerability to being trapped at a local optimal point [20]. PSO has solved a wide range of electrical engineering optimization problems such as parametric optimization of a multi-stage linear quadratic regulator (MSLQR) FACTS controller [24], power system stabilizer (PSS) [25] and PV-battery powered fast electric vehicle charging stations [26].

PSO is inspired by bird flocking and shares similarities with genetic algorithms (GA) [17], [20]. The system is initialized with a random solution for a generated population and looks into the best potential solution. The potential solutions are called particles. These particles fly through the defined vector space to find the optimized solution. PSO overcomes the shortcomings of classical techniques due to fast convergence, decreased population and small iteration size. The fast response of PSO helps the PI controllers to function fast when sudden changes occur at the VSC station. A global best (*gBest*) PSO algorithm is adopted in this paper.

In PSO, particles move in a multi-dimensional space and the position of each particle in the vector space improves using the following [20]:

$$v_{id}^{(t+1)} = w \times v_{id}^{(t)} + c_1 \times Rand_1() \times (pBest_{id} - x_{id}^{(t)}) + c_2 \times Rand_2() \times (gBest_{id} - x_{id}^{(t)}), \quad d = 1, 2, \ldots, M \tag{8}$$

$$x_{id}^{(t+1)} = x_{id}^{(t)} + x \times v_{id}^{(t+1)}, \quad i = 1, 2, \ldots., N \tag{9}$$

where v_{id}^t is the velocity of the i^{th} particle in the t-iteration, x_{id}^t is the dimension of the i^{th} particle in t-iteration. c_1 and c_2 are weight factors of the cognitive and social components, respectively, while w is inertial weight. *pBest* and *gBest* are personal best and global best values for the particles while $Rand_1$ and $Rand_2$ are uniformly distributed random values between 0 to 1.

Operation of the PSO algorithm is illustrated in Fig. 4. PSO parameters are initialized in the first step, which includes the dimension and number of particles. These parameters (dimension of particles) are equivalent to the number of

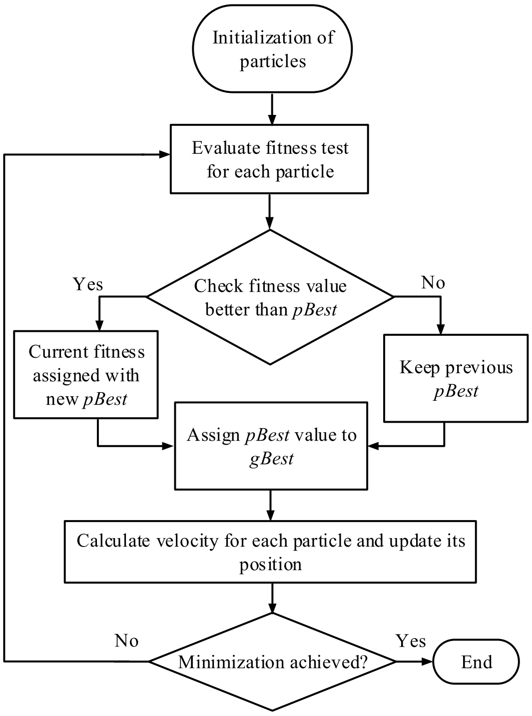

FIGURE 4. Implementation of PSO on VSCs control system.

ambiguous parameters in the given problem. The initial position of the particles is generated and then particle performance is examined. This is achieved by setting the personal best and then the global best for each particle is found using the fitness function of (9). Next velocity and position are updated using (8) and (9), respectively. Every particle updates its personal and global bests until it finds the best solution. The block diagram in Fig. 5 shows the PSO application procedure on the PI controllers.

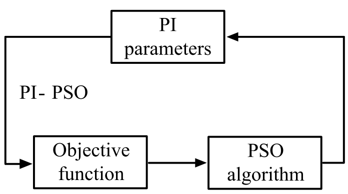

FIGURE 5. Procedure of PSO application on PI controllers.

IV. PSO BASED MULTI-OBJECTIVE OPTIMIZATION of VSC's

The proposed optimization can develop an multi-objective optimization function for the VSC station control parameters. The VSC stations fundamental control layers, ICC and OCL, are tuned optimally in a parallel operation.

A. TUNING OF THE INNER CURRENT CONTROL LAYER

The inner current control loop is the core of the VSCs controller. Improving the PI control parameters using a PSO based multi-objective function is critical for optimal gains. Fig. 6 shows the ICC schematic diagram of the PSO approach. The characterized objective function is:

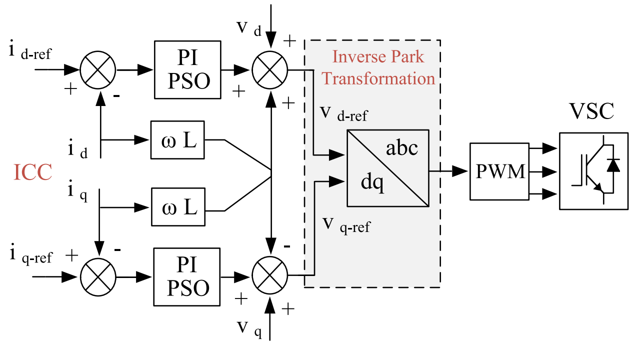

FIGURE 6. Control structure of inner current control using PSO.

$$Minimize: \ O_{ICC} = \int_{0}^{T} t.|id - id, ref|\, dt \tag{10}$$

B. TUNING OF THE OUTER CONTROL LAYER

In the multi-objective function, OCL control parameters are tuned in parallel with ICC parameters, for optimized gains. Fig. 7 shows the PSO implementation in the outer control loop. The characterized OCL objective function is:

$$Minimize: \ O_{OCL} = \int_{0}^{T} t.|P - Pref|\, dt \tag{11}$$

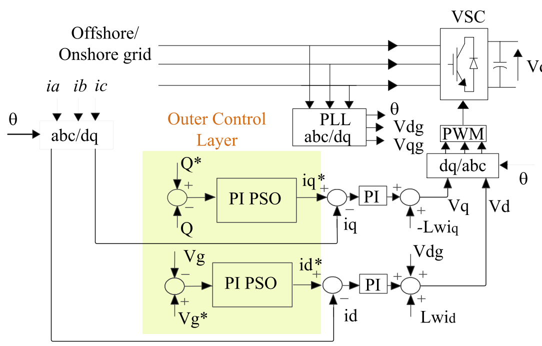

FIGURE 7. Control structure of outer control layer using PSO.

V. IMPLEMENTATION OF MULTI-OBJECTIVE FUNCTION

Simultaneous minimization for the number of objective problems is achieved using the multi-objective function (OB-FN). The objective of this paper, M-HVdc system fast response under dynamic situation, is achieved by minimizing the multi-objective function. Firstly, standard constrained problems are optimized separately and then the active set approach is used to find the best compound solution. Then a weighted sum approach is applied with the PSO algorithm for parallel tuning of the respective objective functions of the ICC and OCL controllers. The control layout for this optimized process is

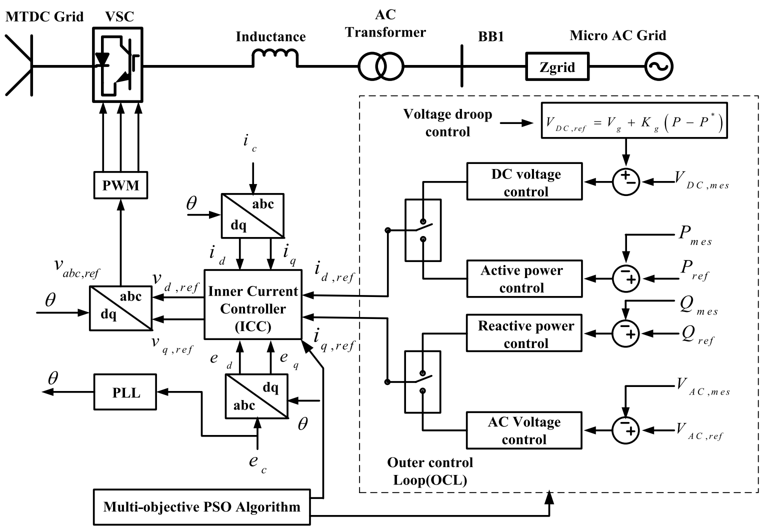

FIGURE 8. PSO based multi-objective tuning of VSCs.

shown in Fig. 8. The selection criterion for weights is user defined and an autonomous generated set of values [27]. The multi-objective problem is considered a compound objective function in the weighted sum technique. The compound objective function can be represented mathematically as:

$$OB - FN = \sum_{j=1} w_j F_j(x) j = 1, 2 \tag{12}$$

where w_j: represent non-zero weight values.

The minimization of (12) helps to obtain the optimization goals of the multi-objective problem. In this case, the objective is to provide a composition consisting of two different objective functions, (10) and (11). The weight of each objective function determines the compromised solution, whereas the weight selection defines the importance of each component in (13). Thus the objective function can be re-written as:

$$OB - FN = w_1 O_{ICC} + w_2 O_{OCL} \tag{13}$$

The weights of w_1 and w_2 are assigned and related according to:

$$w_2 = 1 - w_1 \tag{14}$$

where w_1 is from 0 to 1.

Tuned parameters for the controllers are obtained by adopting the flow chart in Fig. 9. In the first stage, random particles are generated and a weightage set for w_1 and w_2 are designated. Considering the PSO and its initialized particles, the optimal estimations are obtained for the PI control parameters which then validates the minimization of the main objective function (13).

VI. EVALUATION AND COMPARISON OF CONTROLLERS PERFORMANCE

In this section, PI parameters (k_p and k_i) are tuned using both the proposed PSO algorithm considering the minimization

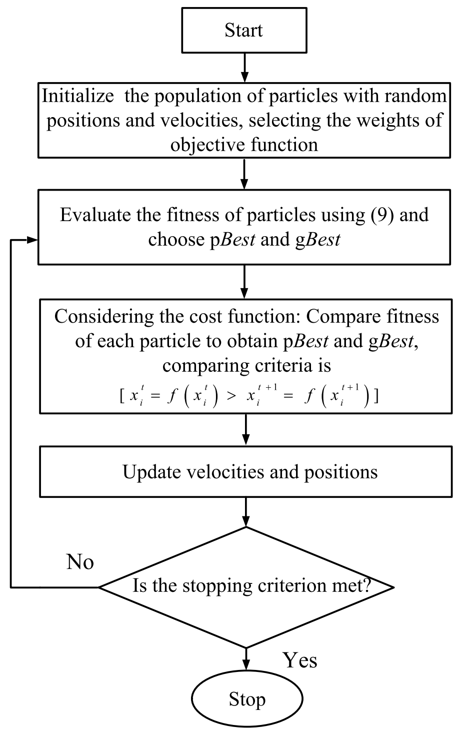

FIGURE 9. Implementation of multi-objective function using weighted sum based PSO.

of the objective function defined in (12) and using classical tuning method. The PSO algorithm parameters are given in Table 2. PSO-optimized parameters are compared with the classically tuned PI (C-PI) parameters. For assessment, parameters from both methods are tested by implementation on the test grid of Fig. 1 via simulations; presented in the subsequent section.

TABLE 2. PSO algorithm parameters.

Specifications	Particles values	Initial population	No. of iterations	w_1 and w_2
Value	04	15	10	0.85 & 0.15

A. ICC TUNING BASED ON CLASSICAL TUNING METHOD

The C-PI control parameters are based on [28] and [29]:

1) To achieve appropriate performance, the closed loop bandwidth of ICC should be 0.2 times less than the switching angular frequency.
2) To obtain a closed loop system free from oscillatory response; ICC controllers should be 10 times faster than the outer controllers.

Thus, PI control parameters for ICC are selected as [30]:

$$K_{p,I} \leq \alpha_c L_T^{pu} \quad (15)$$
$$K_{i,I} \leq \alpha_c R_T^{pu} \quad (16)$$

where α_c is the closed loop bandwidth for ICC and 2kHz is selected switching frequency in this paper. Thus:

$$\alpha_c \leq 2.5 = {}^{4}/_{5}\pi \quad krad/s \quad (17)$$

The 2krad/s is designated for α_c considering safety and margin issues. The ICC parameters are computed and presented in Table 3, based on (15), (16) and Table 2.

TABLE 3. Inner and Outer Control loop parameters obtained using PSO and classical tuning techniques.

Controllers	Classical-PI		PSO-PI	
	k_p	k_i	k_p	k_i
ICC	0.5000	14.9300	0.7786	18.7610
OCL (Power)	0.1000	33.0030	0.7786	73.2660

B. OCL TUNING BASED ON CLASSICAL TUNING METHOD

Similar steps are adopted to tune the OCL parameters, based on the fact that ICC should be 10 times faster than OCL to accomplish non-oscillatory response in the closed loop system. Thus, the bandwidth for the outer layer PI controllers are:

$$\alpha_{oc} \leq 0.1\alpha_c \quad (18)$$

Then k_p and k_i parameters for the OCL controllers are derived based on the concept in [30], and given by:

$$k_{p,O} \leq \alpha_{oc} C^{pu} \quad (19)$$
$$k_{i,O} \leq \alpha_{oc}^2 C^{pu} \quad (20)$$

Classically tuned parameters for the active power controller are given in Table 3, attained by employing (19) and (20).

C. MULTI-OBJECTIVE OPTIMIZATION OF ICC AND OCL USING PSO

Multi-objective optimization based on PSO for inner and outer control layers is carried out for one VSC and then optimized PI parameters are adopted in the other VSCs likewise.

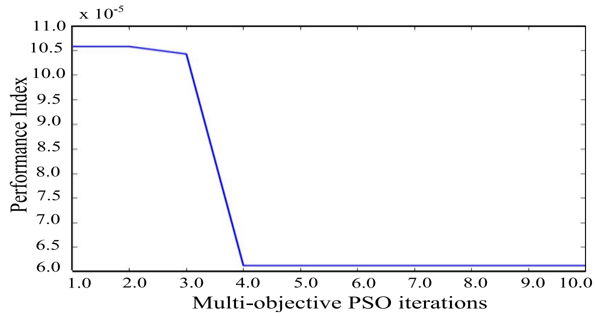

FIGURE 10. Performance of PSO algorithm for multi-objective optimization of VSCs.

PSO particles are initially positioned around the solution of classical tuning. Hence to obtain the optimally tuned k_p and k_i parameters, the PSO algorithm is executed. The values for the fitness function during the PSO based multi-objective optimization are shown in Fig. 10. The values of the ICC and OCL controllers evolve via certain iterations of the algorithm of Fig. 9. This evolution helps to minimize the fitness function which in return provides tuned k_p and k_i values. Tuned PI parameters for ICC and OCL based on PSO and tuning technique of [28] and [29] are given in Table 3.

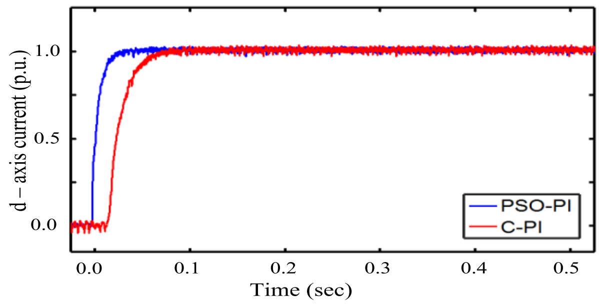

FIGURE 11. Step response of inner current control layer for C-PI and PSO-PI.

To assess the performance of the objective function in the proposed optimization algorithm, a typical step response of ICC is implemented and the results are compared. The step response of the inner control loop for PSO based optimization and C-PI is shown in Fig. 11. The active power profile attained by C-PI and PSO-PI are shown in Fig. 12.

From Fig. 11 and Fig. 12, the PSO-controller exhibits significantly improved performance, explicitly faster rise time than the C-PI controller.

For presenting a sensible numerical assessment for C-PI and PSO-PI controllers' performance, they are compared in terms of the minimization of the integral of time multiplied

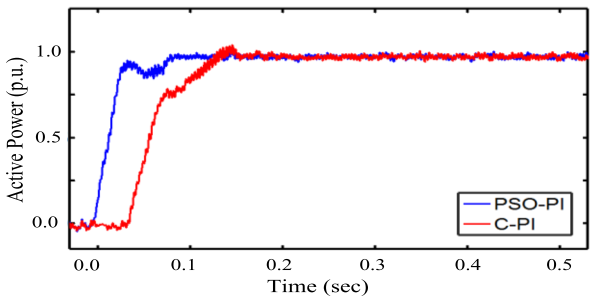

FIGURE 12. Active power profile resulted from C-PIs and PSO-PIs.

TABLE 4. PSO and classically tuned PI controllers comparison in terms of ITAE.

Controllers	ITAE	
	Classical tuned	PSO tuned
ICC	4.7110×10^{-4}	8.4560×10^{-5}
OCL (Power)	1.5601×10^{-3}	5.9750×10^{-4}
OB-FN	-	6.4560×10^{-5}

by absolute error (ITAE) measurements of (10), (11) and (13), in Table 4.

VII. SIMULATION RESULTS

The proposed control structure is evaluated on the four terminal HVdc system of Fig. 1. The dc test system consists of two offshore WFs and two onshore grids. Mainland based VSC stations (MMC-1 and MMC-2) are designed to regulate the dc link voltage via P-Vdc droop and reactive power control [12]. $k_1 = 5$ and $k_2 = 7$ are droop constants. This setting aids the control real power exchange between the dc and ac grids plus maintains constant dc link voltage. MMC-3 and MMC-4 are set to a P-Vac control mode to establish constant real power flow within the dc grid [3], [12] and controls the ac voltage at the PCC. The dc link operates at ±200 kV and the dc grid ratings are given in Table 1.

The test system VSCs are identical since the optimization process is carried out on only one VSC station, with the obtained control parameters implemented on all VSCs. To assess the flexibility and validity of the proposed control, simulations are assessed for three different test scenarios: change in wind power, power demand variations from ac networks, and eventual VSC disconnection.

A. SCENARIO I: CHANGE IN WIND FARM POWER

In first case, power from WF_2 is ramped to 0.6 p.u. from 0.4 p.u. while P_{WF1} remains constant. The dc link voltage increases to 1.02 p.u. via coordinated proportional droop control of the GS-MMCs as the power transfer increases. Power is transmitted to the ac networks through $GS\text{-}MMC_1$ and $GS\text{-}MMC_2$. Real power and dc-link voltage profiles for scenario-1 for both classical and meta-heuristic PSO approaches are shown in Fig. 13. At $t = 1.5$ s, power through WF_1 is raised to 1.0 p.u. while P_{WF2} remains constant and the dc-link voltage settles at 1.04 p.u., using droop control characteristics.

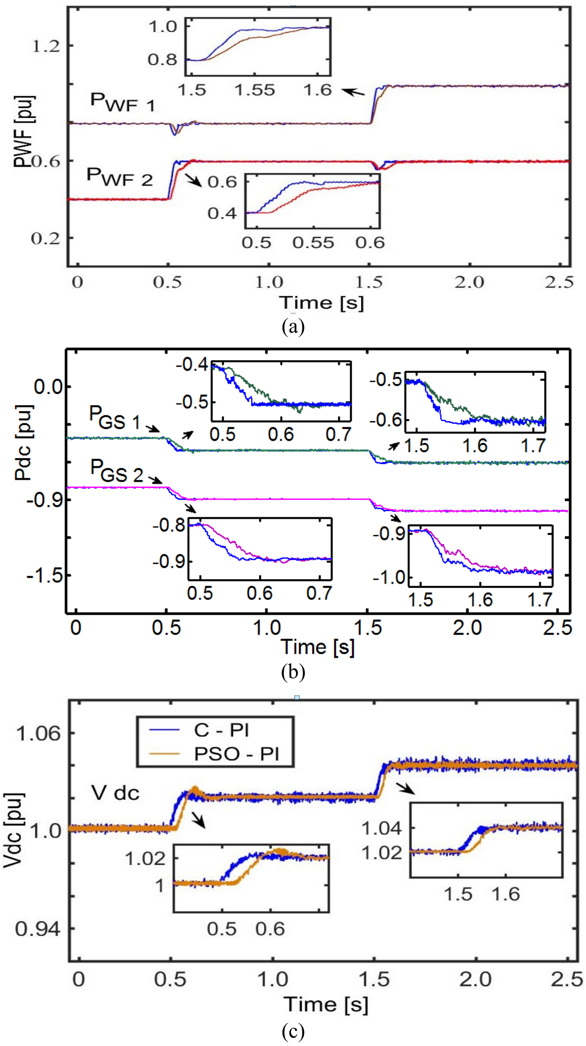

FIGURE 13. Active power and dc voltage during change in power reference from WF_2 and WF_1, respectively. (C-PI: blue lines, PSO-PI: other than blue). (a) Wind farm power profile. (b) Onshore grid power profile. (c) The dc-link voltage profile.

From Fig. 13, the multi-objective PSO-controllers show significant improvement compared to the classical PI. The rise time and stability margins are significantly improved at onshore and offshore stations.

B. SCENARIO II: CHANGE IN LOAD DEMAND

In this scenario, the response of the dc grid is examined when the load demand is increased at time $t = 0.5$s. Due to this sudden change in demand, GS_1 changes its power from -0.4 p.u. to -0.5 p.u. and the implementation of voltage droop control at onshore grids help GS_2 balance the power sharing by adjusting its dc voltage and decreasing its power consumption to -0.7 p.u. A detailed analysis is seen in Fig. 14(b). Similarly, at $t = 1.5$s, when GS_2 decreases its power.

Extracted WF power is shown in Fig. 14 (a). P_{WF1} and P_{WF2} profiles are constant during load demand change on grid side converters at 0.8 p.u. and 0.4 p.u., respectively.

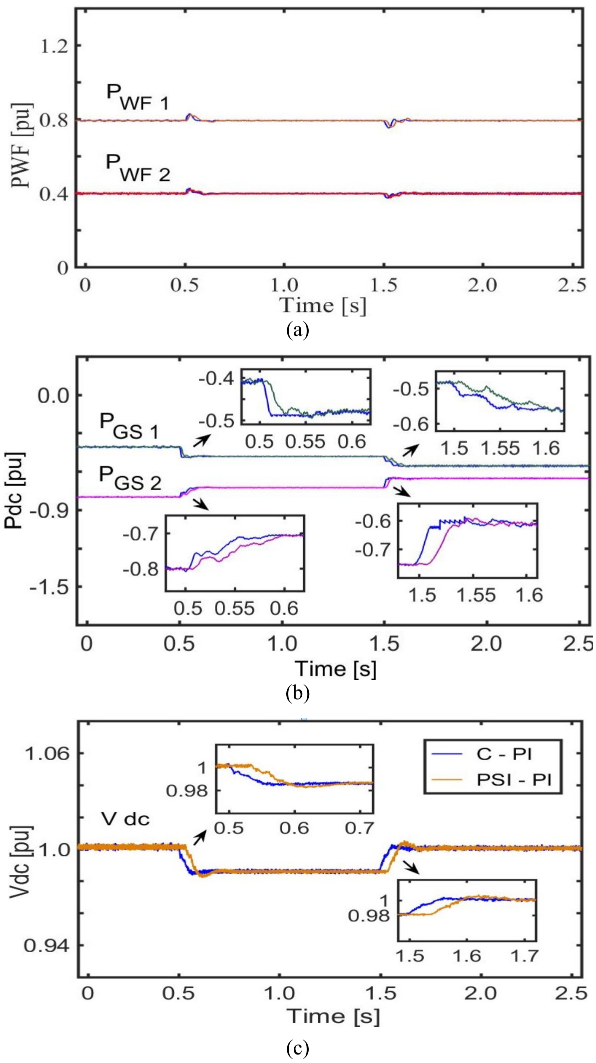

FIGURE 14. Active power and dc voltage during change in power reference from GS_2 and GS_1, respectively. (C-PI: blue lines, PSO-PI: other than blue). (a) Wind farm power profile. (b) Onshore grid power profile. (c) The dc-link voltage profile.

However, it shows bit fluctuation on load change but settles back to its original level.

To show the desirable effects of the proposed technique on grid station, a comparison between classical tuning and PSO algorithm is illustrated in Fig.14. Graphical observation indicates that PSO-optimized parameters stabilize the power and dc voltages profiles much faster than C-PI.

C. SCENARIO III: PERMANENT FAULT AT GS-MMC

A three phase permanent hard fault is applied to evaluate the stability performance of the M-HVdc system. A three phase symmetrical fault is introduced at the GS_1. Before the fault, WF_1 and WF_2 generate total power of 1.0 p.u. and the onshore grids share this power according to their voltage droop characteristics. However, when the fault occurs on GS_1 at time $t = 0.5$s, the generated power expeditiously shifts towards GS_2 and power though GS_1 is reduced to zero.

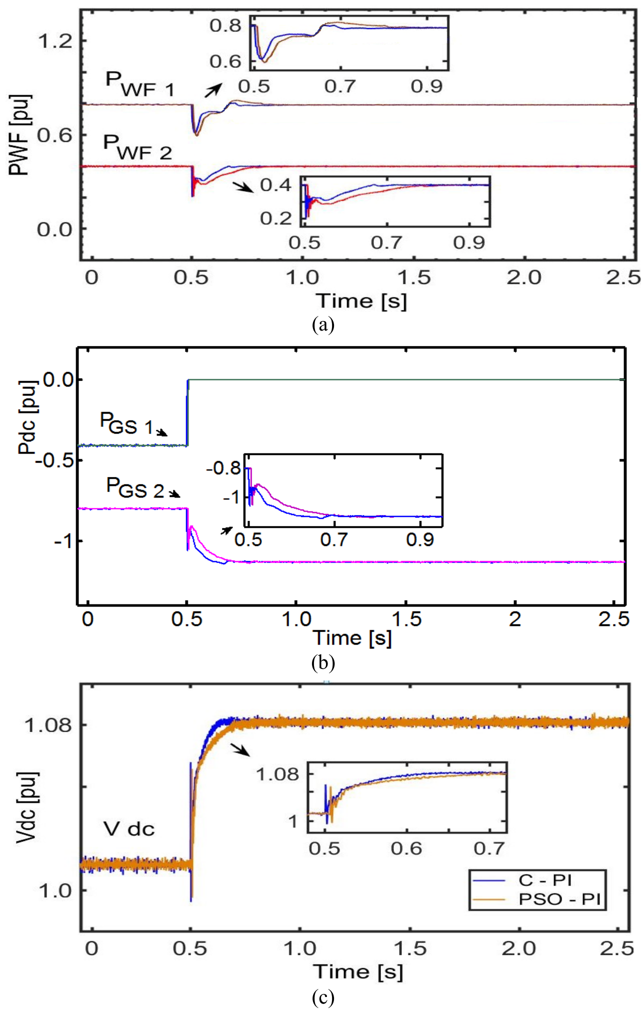

FIGURE 15. Active power and dc voltage during ultimate disconnection of GS_1. (C-PI: blue lines, PSO-PI: other than blue). (a) Wind farm power profile. (b) Onshore grid power profile. (c) The dc-link voltage profile.

Graphical analysis of Fig. 15 (a) indicates that at the fault occurrence instant, offshore grids show marginal effects in their power generations and quickly return to their normal state. Meanwhile, GS_2 controlled parameters enable the power and dc-link voltage to quickly attain the required output levels. Clearly, PSO based controllers shows faster response than C-PI controllers. The dc link voltage stabilize itself within $\pm 10\%$ suggested limit in [31], during all three scenarios which proves that the proposed control algorithm works well.

Optimized VSC stations based on PSO-multi-objective may also find its application in centralized voltage source converters (CVSC) connected offshore wind turbines (WTs) to enhance energy extraction. An optimal power extraction (OPE) strategy based on the proposed optimization technique can effectively improve the energy extraction efficiency of the traditional CVSCs-WTs.

VIII. CONCLUSION

Multi-objective optimization based on a meta-heuristic technique, particle swarm optimization, was presented to tune the control parameters of VSC stations in M-HVdc grids. The ICC and OCL PI controllers were optimized, simultaneously, via the proposed multi-objective PSO algorithm to realize desirable VSC dynamic performance. Then, the optimized control parameters were implemented in a four terminal VSC-HVdc test grid to assess control performance. Test rig simulations used PSCAD/EMTDC. For comparison, classical optimization technique was also implemented in same environment as proposed algorithm. The simulated workbench was assessed for: (i) load demand change from the ac grids, (ii) wind power change, and (iii) eventual permanent VSC disconnection; for both classical and proposed multi-objective optimization methods. Results established that during both steady and dynamic states multi-objective PSO-controllers show significant improvement and control performance when compared to classical PI controllers. The rise time and stability margins are significantly improved both at onshore and offshore stations.

ACKNOWLEDGMENT

The authors are grateful to Prof. Barry W. Williams, University of Strathclyde, UK for reviewing and proof reading the manuscript, both technically and linguistically.

REFERENCES

[1] J. Blau, "Europe plans a North Sea grid," *IEEE Spectr.*, vol. 47, no. 3, pp. 12–13, Mar. 2010.

[2] R. Irnawan, F. F. da Silva, C. L. Bak, and T. C. Bregnhøj, "An initial topology of multi-terminal HVDC transmission system in Europe: A case study of the North-Sea region," in *Proc. IEEE Int. Energy Conf. (ENERGYCON)*, Leuven, Belgium, Apr. 2016, pp. 1–6.

[3] L. Jun, J. Tianjun, O. Gomis-Bellmunt, J. Ekanayake, and N. Jenkins, "Operation and control of multiterminal HVDC transmission for offshore wind farms," *IEEE Trans. Power Del.*, vol. 26, no. 4, pp. 2596–2604, Oct. 2011.

[4] D. Van Hertem and M. Ghandhari, "Multi-terminal VSC HVDC for the European supergrid: Obstacles," *Renew. Sustain. Energy Rev.*, vol. 14, no. 9, pp. 3156–3163, Dec. 2010.

[5] K. Rouzbehi, J. I. Candela, A. Luna, G. B. Gharehpetian, and P. Rodriguez, "Flexible control of power flow in multiterminal dc grids using DC–DC converter," *IEEE J. Emerg. Sel. Topics Power Electron.*, vol. 4, no. 3, pp. 1135–1144, Sep. 2016.

[6] K. Rouzbehi, A. Miranian, J. I. Candela, A. Luna, and P. Rodriguez, "A generalized voltage droop strategy for control of multiterminal DC grids," *IEEE Trans. Ind. Appl.*, vol. 51, no. 1, pp. 607–618, Jan./Feb. 2015.

[7] K. Rouzbehi, W. Zhang, J. I. Candela, A. Luna, and P. Rodriguez, "Unified reference controller for flexible primary control and inertia sharing in multi-terminal voltage source converter-HVDC grids," *IET Gener., Transmiss. Distrib.*, vol. 11, no. 3, pp. 750–758, Feb. 2017.

[8] H. Rao, "Architecture of Nan'ao multi-terminal VSC-HVDC system and its multi-functional control," *CSEE J. Power Energy Syst.*, vol. 1, no. 1, pp. 9–18, Mar. 2015.

[9] Y. Y. Li, X. M. Huang, J. Zhang, and W. Z. Sun. (Aug. 2017). *China Upgrades Capacity to the Zhoushan Islands: State Grid Corporation Installs First HVDC Five-Terminal Voltage Source Converter Project*. [Online]. Available: http://www.tdworld.com/digital-innovations/chinaupgrades-capacity-zhoushan-islands

[10] G. Wu *et al.*, "Analysis and design of vector control for VSC-HVDC connected to weak grids," *CSEE J. Power Energy Syst.*, vol. 3, no. 2, pp. 115–124, Jun. 2017.

[11] K. Rouzbehi, A. Miranian, J. I. Candela, A. Luna, and P. Rodriguez, "A hierarchical control structure for multi-terminal VSC-based HVDC grids with GVD characteristics," in *Proc. Int. Conf. Renew. Energy Res. Appl. (ICRERA)*, Madrid, Spain, Oct. 2013, pp. 996–1001.

[12] A. Raza, X. Dianguo, L. Yuchao, S. Xunwen, B. W. Williams, and C. Cecati, "Coordinated operation and control of VSC based multiterminal high voltage DC transmission systems," *IEEE Trans. Sustain. Energy*, vol. 7, no. 1, pp. 364–373, Jan. 2016.

[13] Z.-L. Gaing, "A particle swarm optimization approach for optimum design of PID controller in AVR system," *IEEE Trans. Energy Convers.*, vol. 19, no. 2, pp. 384–391, Jun. 2004.

[14] R. A. Krohling and J. P. Rey, "Design of optimal disturbance rejection PID controllers using genetic algorithms," *IEEE Trans. Evol. Comput.*, vol. 5, no. 1, pp. 78–82, Feb. 2001.

[15] T. L. Seng, M. B. Khalid, and R. Yusof, "Tuning of a neuro-fuzzy controller by genetic algorithm," *IEEE Trans. Syst. Man, Cybern. B, Cybern.*, vol. 29, no. 2, pp. 226–236, Apr. 1999.

[16] E. Song, A. F. Lynch, and V. Dinavahi, "Experimental validation of nonlinear control for a voltage source converter," *IEEE Trans. Control Syst. Technol.*, vol. 17, no. 5, pp. 1135–1144, Sep. 2009.

[17] F. B. David, *Evolutionary Computation: Toward a New Philosophy of Machine Intelligence*, 3rd ed. Hoboken, NJ, USA: Wiley, Apr. 2006.

[18] L. H. Hassan, M. Moghavvemi, H. A. F. Almurib, and K. M. Muttaqi, "A coordinated design of PSSs and UPFC-based stabilizer using genetic algorithm," *IEEE Trans. Ind. Appl.*, vol. 50, no. 5, pp. 2957–2966, Sep. 2014.

[19] M. E. Lotfy, T. Senjyu, M. A. Farahat, A. F. Abdel-Gawad, and A. Yona, "Enhancement of a small power system performance using multi-objective optimization," *IEEE Access*, vol. 5, pp. 6212–6224, 2017.

[20] J. Kennedy and R. Eberhart, "Particle swarm optimization," in *Encyclopedia of Machine Learning*. Boston, MA, USA: Springer, 2011, pp. 760–766. [Online]. Available: https://link.springer.com/referenceworkentry/10.1007/978-1-4899-7687-1_630#howtocite

[21] F. M. de Oliveira, S. A. O. da Silva, F. R. Durand, L. P. Sampaio, V. D. Bacon, and L. B. G. Campanhol, "Grid-tied photovoltaic system based on PSO MPPT technique with active power line conditioning," *IET Power Electron.*, vol. 9, no. 6, pp. 1180–1191, 2016.

[22] Y.-B. Wang *et al.*, "Acoustic localization of partial discharge sources in power transformers using a particle-swarm-optimization-route-searching algorithm," *IEEE Trans. Dielectr. Electr. Insul.*, vol. 24, no. 6, pp. 3647–3656, Dec. 2017.

[23] L. Xu, "Modeling, analysis and control of voltage-source converter in microgrids and HVDC," M.S. thesis, Univ. South Florida, Tampa, FL, USA, Nov. 2013.

[24] R. K. Pandey and D. K. Gupta, "Integrated multi-stage LQR power oscillation damping FACTS controller," *CSEE J. Power Energy Syst.*, vol. 4, no. 1, pp. 83–91, Mar. 2018.

[25] D. Ke, F. Shen, C. Y. Chung, C. Zhang, J. Xu, and Y. Sun, "Application of information gap decision theory to the design of robust wide-area power system stabilizers considering uncertainties of wind power," *IEEE Trans. Sustain. Energy*, vol. 9, no. 2, pp. 805–817, Apr. 2018.

[26] M. O. Badawy and Y. Sozer, "Power flow management of a grid tied PV-battery system for electric vehicles charging," *IEEE Trans. Ind. Appl.*, vol. 53, no. 2, pp. 1347–1357, Mar./Apr. 2017.

[27] R. T. Marler and J. S. Arora, "The weighted sum method for multi-objective optimization: New insights," *Struct. Multidisciplinary Optim.*, vol. 41, no. 6, pp. 853–862, Jun. 2010.

[28] K. Rouzbehi, A. Miranian, A. Luna, and P. Rodriguez, "Optimized control of multi-terminal DC grids using particle swarm optimization," *Eur. J. Power Electron.*, vol. 24, no. 2, pp. 38–49, 2014.

[29] R. T. Pinto, P. Bauer, S. F. Rodrigues, E. J. Wiggelinkhuizen, J. Pierik, and B. Ferreira, "A novel distributed direct-voltage control strategy for grid integration of offshore wind energy systems through MTDC network," *IEEE Trans. Ind. Electron.*, vol. 60, no. 6, pp. 2429–2441, Jun. 2013.

[30] S. Rodrigues, "A multi-objective optimization framework for the design of offshore wind farms," Ph.D. dissertation, Delft Univ. Technol., Delft, The Netherlands, 2016.

[31] J. Beerten, S. Cole, and R. Belmans, "Modeling of multi-terminal VSC HVDC systems with distributed DC voltage control," *IEEE Trans. Power Syst.*, vol. 29, no. 1, pp. 34–42, Jan. 2014.

ALI RAZA received the B.S. and M.Sc. degrees in electrical engineering from the University of Engineering and Technology, Lahore, Pakistan, in 2010 and 2013, respectively, and the Ph.D. degree in electrical engineering from the Harbin Institute of Technology, Harbin, China, in 2016. He is currently with the Department of Robotics and AI, National University of Sciences and Technology, Pakistan, and also with the Department of Electrical Engineering, University of Lahore, Pakistan. He has authored and co-authored several technical journal papers and technical conference proceedings. His research interests include operation and control of M-VSC-HVDC, including its effects on power systems, including protection, optimization, and topological evaluation of MT-HVDC transmission systems for large offshore wind power plants. He serves as reviewer for the multiple IEEE Transactions and Elsevier Journals.

Dr. Raza has been a TPC member of the International Symposium on Wireless Systems and Networks since 2017. He received the First Best Paper Award from the 2014 IEEE International Conference on Control Science and Systems Engineering. He is the Co-Chair of the Asia Pacific International Conference on Electrical Engineering 2019 (APICEE 2019).

ZAIN YOUSAF received the B.Eng. degree in electronics and electrical engineering from Swansea University, U.K., in 2014, the M.Sc. degree in electrical engineering from The University of Lahore, Pakistan. He is currently with the Department of Robotics and AI, National University of Sciences and Technology, Islamabad. His area of interest includes the power system optimization and control strategy and protection of multi-terminal DC transmission systems.

MOHSIN JAMIL received the B.Eng. degree in industrial electronics from NED University, Pakistan, in 2004, the M.Sc. degree in electrical engineering from Dalarna University, Sweden, in 2006, and the Ph.D. degree from the University of Southampton, U.K., in 2011. He is currently an Assistant Professor with the Department of Robotics and AI, National University of Sciences and Technology, Islamabad, Pakistan. He has authored a book chapter and several IEEE publications. His research interests include control design, multi-terminal HVdc transmission systems, soft switching techniques, and smart grid technologies.

SYED OMER GILANI received the M.Sc. degree in computer engineering in Sweden in 2006 and the Ph.D. degree in electrical and computer engineering from the National University of Singapore in 2013. From 2006 to 2008, he was with the Interactive Multimedia Lab, Singapore. He is currently an Assistant Professor with the National University of Sciences and Technology, Pakistan. His research interests include use of power electronic in power systems, multi-terminal HVdc transmission systems, human–machine interaction and networking and, actively consult for industry on various projects.

GHULAM ABBAS received the B.E. degree from the University of Engineering and Technology, Lahore, Pakistan, in 2004, and the M.E. and the Ph.D. degrees from the Institut National des Sciences Appliquées de Lyon, France, in 2008 and 2012, respectively, all in electrical engineering. He is currently with the Department of Electrical Engineering, The University of Lahore, Pakistan. He has published a number of papers in various IEEE conferences and international journals. His research interests include analog and digital controller designs for power switching converters, and power system optimization.

MUHAMMAD UZAIR received the bachelor's degree in electrical engineering from the University of Engineering and Technology, Lahore, Pakistan, in 1996, the master's degree from Concordia University, Montreal, in 2005, and the Ph.D. degree from the University of Guelph, Guelph, ON, Canada, in 2014, all in electrical engineering. He was an Electronics/Instrument Engineer for five years in the biomedical and petrochemical industry in Pakistan. He has been an Assistant Professor with the Faculty of Engineering, Islamic University of Madinah, Madinah, Saudi Arabia, since 2016. His research interests include image/video and signal processing, developing algorithms for solving engineering problems and medical applications, and developing wireless protocols, and wireless video optimization.

SAIMA SHAHEEN received the B.S. and M.Sc. degrees in electrical engineering from the University of Engineering and Technology, Lahore, Pakistan, in 2010 and 2016, respectively. She is currently with the Department of Electrical Engineering, University of Management and Technology, Pakistan. Her area of interest is operation and control of multi-terminal VSC-HVDC transmission systems.

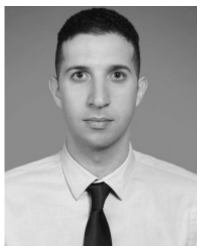

ABDELDJABAR BENRABAH was born in Skikda, Algeria, in 1988. He received the Engineering degree in electrical engineering from the Ecole Militaire Polytechnique, Algiers, Algeria, in 2012, and the Ph.D. degree in electrical engineering from the Harbin Institute of Technology, Harbin, China, in 2018. He is currently with the Electrical Engineering Department, Ecole Militaire Polytechnique, as a Post-Doctoral Research Fellow. His research interests include the control of grid connected converters, multi-terminal VSC-HVdc systems, renewable energy, and microgrids. He was a recipient of the Chinese Government Outstanding International Student Scholarship in 2017.

FAJUN LI received the B.E. degree in physics from the North University of China in 2010 and the master's degree in optics in 2012. He is currently pursuing the Ph.D. degree with the Department of Electronic Science and Technology, Harbin Institute of Technology. He has been a Visiting Scholar with the Australian National University for one and half years since 2014. His research interests include control design, multi-terminal HVdc transmission systems, and soft switching techniques.